

MAGNETIC ACCRETION ONTO T TAURI STARS

Christopher M. Johns–Krull

Physics & Astronomy Dept., Rice University, Houston, TX, USA

Jeff A. Valenti

Space Telescope Science Institute, Baltimore, MD, USA

and

April D. Gafford

Physics & Astronomy Dept., San Francisco State University, San Francisco, CA, USA

RESUMEN

Espectroscopía de alta resolución de líneas de absorción fotosféricas, particularmente en el infrarrojo, revelan la presencia de campos magnéticos en las estrellas T Tauri. Espectropolarimetría de alta resolución restringe la geometría de los campos magnéticos estelares de gran escala, que se supone juegan un papel crucial en controlar la acreción y eyección de vientos en estos sistemas. Revisamos las más recientes mediciones de campos magnéticos en estrellas T Tauri, que ofrecen evidencia de la importancia de los campos magnéticos estelares en el control de la acreción de material, y comparamos las mediciones con las predicciones de la teoría.

ABSTRACT

High resolution spectroscopy of photospheric absorption lines, particularly in the infrared, reveals the presence of magnetic fields on T Tauri stars. High resolution circular spectropolarimetry provides strong constraints on the geometry of the large scale stellar magnetic fields believed to play a crucial role in controlling accretion onto, and winds from, these stars. We review the latest measurements of T Tauri magnetic fields, which show convincing evidence that stellar magnetic fields do control accretion onto the star. We then compare the measurements with expectations from theory.

Key Words: **ACCRETION : DISKS — STARS: MAGNETIC FIELDS — STARS: PRE-MAIN SEQUENCE**

1. INTRODUCTION

T Tauri stars (TTS) are newly born, roughly solar mass stars that have only recently emerged from their parent molecular cloud cores to become optically visible. Recently, both theoretical and observational work appear to be converging on a coherent picture of TTS phenomena with the circumstellar disk and strong stellar magnetic fields playing a crucial role. Classical TTS (CTTS) are surrounded by active accretion disks, and directly or indirectly, most of the excess emission seen in these stars can be attributed to the presence of the disk interacting with a magnetically active star (see review by Bertout 1989). This interaction is generally referred to as *magnetospheric accretion*. The model posits that CTTS possess strong stellar magnetic fields which truncate the surrounding accretion disk, forcing accreting material to flow along the stellar field lines to the surface of the star, impacting

preferentially at high latitudes (Uchida & Shibata 1984; Bertout, Basri, & Bouvier 1988; Camenzind 1990; Königl 1991; Cameron and Campbell 1993; Shu et al. 1994). The Shu et al. (1994) model combines this concept of magnetospheric accretion with a model of a magnetocentrifugally driven wind from the truncation point in the disk, thereby elegantly linking mass accretion and outflow in these stars. This unified model of winds and accretion flows in CTTS has become very popular in the star/planet formation community. Despite this great popularity, there remains relatively little knowledge concerning the strength, extent, and geometry of the magnetic fields on TTS, which is the key ingredient in all of the current models of the star-disk interaction for CTTS.

Johns–Krull, Valenti, and Koresko (1999b) examined 3 of the more detailed versions of the magnetospheric accretion theories and showed that they can

be used to predict magnetic field strengths (ranging up to 10 kG) for several CTTS. Such large field strengths are quite detectable with current techniques. Furthermore, magnetic field measurements on CTTS provide a means for quantitatively testing current magnetospheric accretion theories since all of the relevant quantities for a given system can be determined. The general model of magnetically controlled accretion onto a central source is quite popular in astrophysics, showing up for most types of compact objects: white dwarfs (e.g. AM Her stars – Wickramasinghe & Ferrario 2000), pulsars (pulsating X-ray sources – Ghosh & Lamb 1979), and possibly black holes at the center of active galactic nuclei (e.g. Koide, Shibata, & Kudoh 1999). Detailed tests of magnetospheric accretion theory are necessary for understanding CTTSs as well as these other classes of objects.

1.1. The Zeeman Effect

Virtually all measurements of stellar magnetic fields make use of the Zeeman effect. Typically, one of two general Zeeman characteristics are utilized: (1) Zeeman broadening of magnetically sensitive lines observed in intensity spectra, or (2) circular polarization of magnetically sensitive lines. When an atom is in a magnetic field, different projections of the total orbital angular momentum are no longer degenerate, shifting the energy levels participating in the transition. In the simple Zeeman effect, a spectral line splits into 3 components: two σ components split to either side of the nominal line center and one unshifted π component. The wavelength shift of a given σ component is given by $\Delta\lambda = k\lambda^2gB$; where k is a constant, g is the Landé g-factor of the specific transition, B is the strength of the magnetic field, and λ is the wavelength of the transition. One thing to note from this equation is that the λ^2 dependence of the Zeeman effect differs from the λ dependence of Doppler line broadening mechanisms, meaning that observations in the infrared (IR) are generally more sensitive to the presence of magnetic fields than optical observations.

In the ideal case of a two component atmosphere (some fraction of the surface with a magnetic field of a single value; the rest with no field), the observed line profile can be expressed as $F(\lambda) = F_B(\lambda) * f + F_Q(\lambda) * (1 - f)$; where F_B is the spectrum formed in magnetic regions, F_Q is the spectrum formed in non-magnetic regions, and f is the flux weighted surface filling factor of magnetic regions. The magnetic spectrum, F_B , differs from the spectrum in the quiet region not only due to Zeeman

broadening of the line, but also because magnetic fields affect atmospheric structure, causing changes in both line strength and continuum intensity at the surface. Most studies *assume* that the magnetic atmosphere is in fact the same as the quiet atmosphere; a point in need of future work. If the stellar magnetic field is very strong, the splitting of the σ components is a substantial fraction of the line width, and it is easy to see resolved σ components on either side of a magnetically sensitive line. In this case, it is relatively straightforward to measure the magnetic field strength, B , from the splitting, and the depth of the σ components relative to the π component gives the filling factor, f . Errors in the magnetic atmosphere primarily affect f , since B depends on the splitting of the components, not their relative contrast. If the splitting is a small fraction of the intrinsic line width, then the resulting observed profile is only subtly different from the profile produced by a star with no magnetic field and more complicated modelling is required to be sure all possible non-magnetic sources (e.g. rotation and pressure broadening) have been properly constrained. Zeeman broadening observations demonstrate that idealized two-component models do not apply to TTS, which have a distribution of field strengths. Instead, the observed profile can be described by the superposition: $F(\lambda) = \Sigma[F_{B_i}(\lambda) * f_i] + F_Q(\lambda) * (1 - \Sigma f_i)$, where now the f_i are the filling factors for different field strengths, B_i . In the case of strong fields, this can lead to broadened spectral lines which do not show discrete σ components (e.g. Figure 1).

In addition to directly measuring changes in line profile shape produced by the Zeeman effect, it is also possible to simply use line equivalent widths to measure the field. The splitting of the σ components in optically thick lines adds opacity to the line, thereby enhancing the equivalent width (EW). The level of EW enhancement depends on the full Zeeman pattern (most lines are not simple triplets) of the line, the magnetic field strength, and the inherent strength of the line (Basri, Marcy, & Valenti 1992; Guenther et al. 1999). This EW technique is usable at lower spectral resolution and in cases where the magnetic splitting is a small fraction of the intrinsic line width (due to rotation for example); however, as Basri et al. (1992) discuss, the method is very sensitive to errors in the effective temperature and other stellar atmospheric parameters used to model the observed spectrum. The method must be used with caution.

Measuring circular polarization in magnetically sensitive lines is a more direct means of detecting

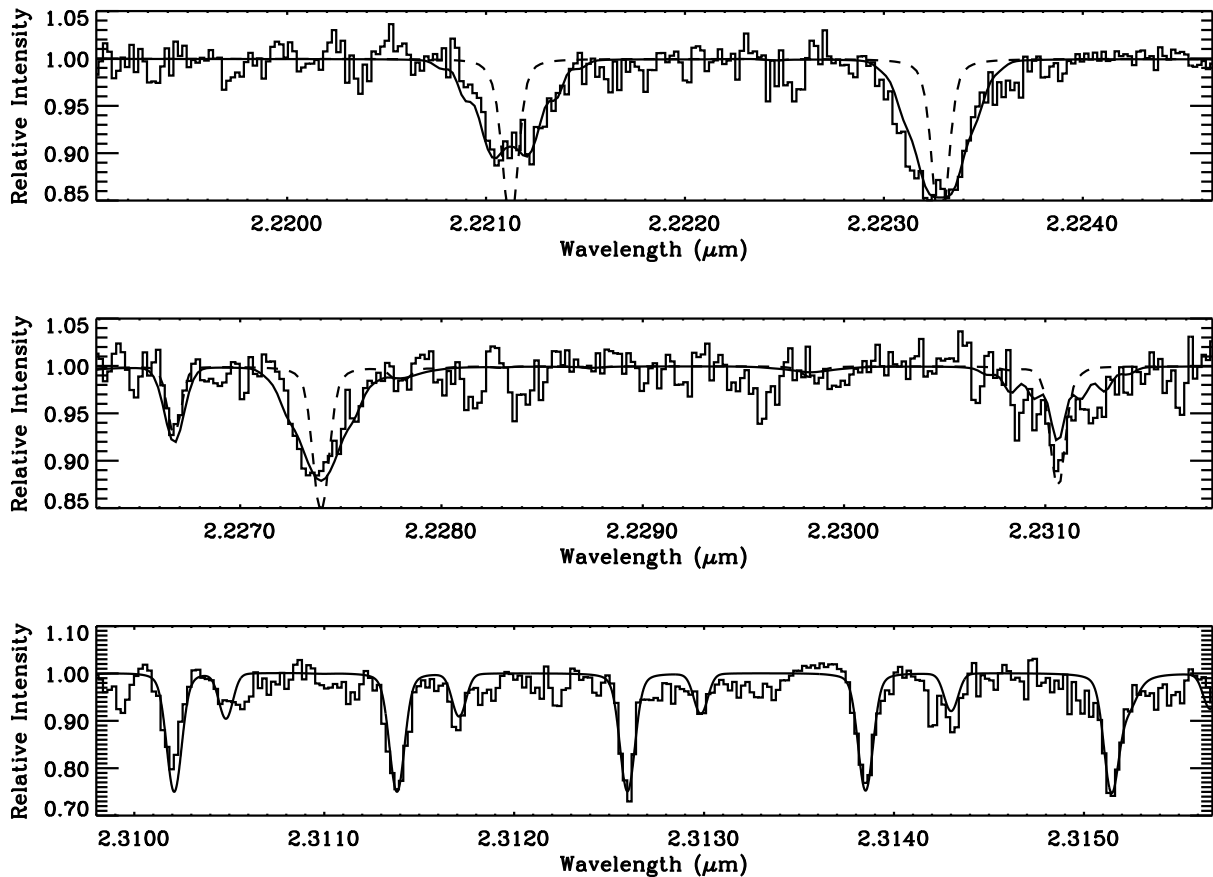


Fig. 1. The black histogram shows three K band spectra of the CTTS TW Hya (4 Ti I lines in the top two panels, and 9 CO lines in the bottom panel). The dashed line is a synthetic spectrum with no magnetic field, and the smooth solid line is the best fitting magnetic model with $\Sigma Bf = 2.6$ kG.

magnetic fields on stellar surfaces, but is also subject to several limitations. When viewed along the axis of a magnetic field, the two σ components are circularly polarized, but with opposite helicity; and the π component is absent. The helicity of the σ components reverses as the polarity of the field reverses. Thus, on a star like the Sun that typically displays equal amounts of + and - polarity fields on its surface, the net helicity is very small. If one magnetic polarity does dominate the visible surface of the star, net circular polarization is present in Zeeman sensitive lines, resulting in a wavelength shift between the line observed through right- and left-circular polarizers. The magnitude of the shift represents the surface averaged line of sight component of the magnetic field (which on the Sun is typically less than 2 G even though individual magnetic elements on the solar surface range from 1.5 kG in plage to ~ 3.0 kG in spots). While polarimetry has been used very successfully to observe the fields on magnetic

Ap stars (globally organized dipole fields ranging up to 34 kG in strength), several polarimetric studies of cool stars and have generally failed to detect circular polarization, placing limits of 10 – 100 G on the disk averaged magnetic field strength (e.g. Vogt 1980; Brown & Landstreet 1981; Borra, Edwards, & Mayor 1984). One notable exception is the detection of circular polarization in segments of the observed line profiles for rapidly rotating RS CVn stars where Doppler broadening of the line “resolves” several independent strips on the stellar surface (e.g. Donati et al. 1997).

1.2. Previous Work on T Tauri Stars

TTS generally rotate rapidly ($v \sin i > 10$ km s^{-1}), making direct detection of Zeeman broadening of optical absorption lines more challenging. The first detection of a photospheric magnetic field on a TTS was made by Basri et al. (1992) utilizing the EW technique. These authors derived a total

magnetic flux of $Bf = 1.0 \pm 0.5$ kG for the naked (non-accreting) TTS (NTTS) Tap 35. Basri et al. (1992) found no systematic enhancement of the magnetically sensitive lines in the NTTS Tap 10, placing an upper limit of $Bf < 0.7$ kG. The relatively large error bars on this measurement result from the fact that the observations were made in the optical, where the Zeeman effect is relatively weak, and also because numerous other atmospheric parameters (e.g. temperature) can strongly affect line equivalent widths. Guenther et al. (1999) apply this same technique to 5 additional TTS, probably detecting fields on two stars, though the systematic effects of stellar atmospheric parameters was not explored for their individual target stars.

Johns-Krull et al. (1999b) analyzed high resolution ($R = 60,000$) optical and IR ($R \sim 35,000$) K band spectra of the CTTS BP Tau. The optical spectra were used to accurately measure the stellar atmospheric parameters of BP Tau, and the IR spectra of a Zeeman sensitive Ti I line clearly showed excess line broadening, which was modeled with a distribution of magnetic field strengths with a total flux $\Sigma Bf = 2.6$ kG.

A key assumption made in all current magnetospheric accretion models is that the stellar magnetic field on TTS is dominated by a dipole component. Such a globally organized field should be detectable via spectropolarimetry; however, early such studies of TTS generally did not have the sensitivity required to detect the proposed fields (see Johns-Krull et al. 1999b). Johns-Krull et al. (1999a) analyzed high resolution ($R = 60,000$) circular spectropolarimetry of the CTTS BP Tau. These data placed an upper limit of 200 G on the mean longitudinal field present in the photosphere, well below current predictions in all but the most unfavorable alignments of the magnetic axis. Quite surprisingly, Johns-Krull et al. (1999a) did detect significant polarization in the He I 5876 Å emission line (Figure 2) which forms in shocks created when accreting disk material impacts the stellar surface. The derived field from the He I line is 2.46 ± 0.12 kG, independent of assumptions regarding the thermal structure of the accretion shock atmosphere.

While these recent investigations have been successful at detecting magnetic fields on TTS, the sample of studied stars is quite small, and insufficient to quantitatively test magnetospheric accretion theories. Over the past few years, we have been engaged in an effort to measure the magnetic field strength on a large sample of TTS in order to quantitatively test current magnetospheric accretion theories. We

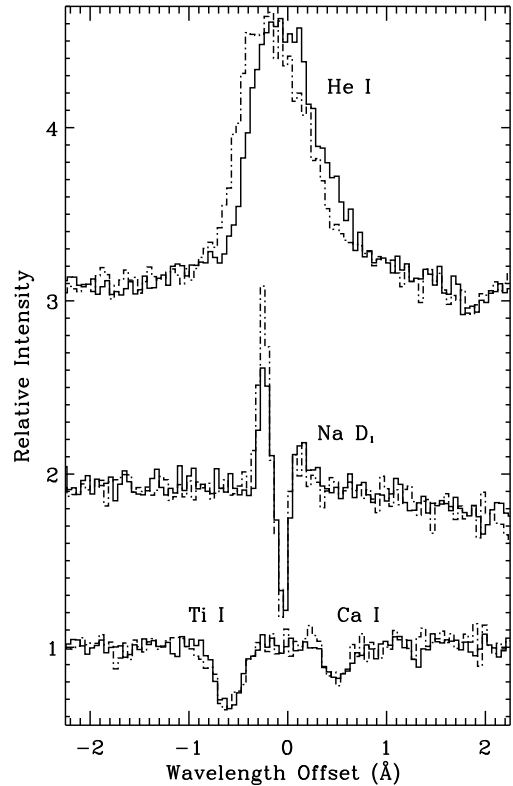


Fig. 2. Three sections of the spectrum of BP Tau in the same order as the He I 5876 Å line. The top two lines have been offset by 1.0 and 2.0 respectively. The solid line is the RCP spectrum and the dash-dot is the LCP spectrum. All profiles are from the same exposure. Note the obvious shift in the two polarizations of the He I line compared to the other lines.

have also engaged in time resolved spectropolarimetry of CTTS in order to explore the geometry of the magnetic fields governing accretion onto these stars. We briefly report on these studies here.

2. RECENT OBSERVATIONS

High resolution ($R \sim 35,000$) K-band spectra of a half-dozen TTS were made at the IRTF on 14 – 20 December 1997, using the CSHELL 1 – 5 μm echelle spectrometer (Tokunaga et al. 1990, Greene et al. 1993). More recently, an additional 12 stars were observed at the IRTF using CSHELL on 7 – 12 January 2000, though these data have not been analyzed in detail. Each star was observed in 4 wavelength settings: 2 settings containing a total of 4 magnetically sensitive Ti I lines, 1 setting containing two weakly magnetically sensitive Na I lines, and 1 setting containing 9 magnetically insensitive CO lines.

In addition to the IR observations, high resolu-

tion ($R = 60,000$) circular spectropolarimetry of 4 CTTS was obtained each night on 23 – 30 November 1998, using the 2.7-m Harlan J. Smith Telescope at McDonald Observatory. As described in Johns-Krull et al. (1999a), a Zeeman analyzer (ZA – Vogt, Tull & Kelton 1980) is used in front of the entrance slit to the cross dispersed, coudé echelle spectrometer at the 2.7-m telescope (Tull et al. 1995). The ZA splits the incoming beam into two parallel beams offset from one another along the spectrograph slit. One beam contains the RCP component of the spectrum and the other the LCP component. Both components are recorded simultaneously on the CCD.

3. ANALYSIS

3.1. CSHELL Analysis

For each TTS, we analyze 4 magnetically sensitive Ti I lines in the K band as well as 9 magnetically insensitive CO lines at $2.3 \mu\text{m}$. For the CTTS BP Tau and the NTTS Hubble 4 we follow Johns-Krull et al. (1999b) and fit high resolution optical spectra with synthetic models to determine key atmospheric parameters (T_{eff} , gravity, $v \sin i$, $[M/H]$) using state of the art stellar atmospheres (Hauschildt et al. 1999). For the other stars, we take literature values of these key atmospheric parameters. Again using model atmospheres from Hauschildt et al. (1999), synthetic line profiles were fit to the K band spectra of the Ti I and CO lines to determine the photospheric magnetic field properties. As found by Johns-Krull et al. (1999b), a single magnetic component added to a non-magnetic component is inadequate to model the data. Therefore, we fit the observed spectra with a distribution of magnetic components with B ranging from 0 - 6 kG in 2 kG steps. For the CTTS, a constant level of pure continuum emission from the disk is also determined. It is important to realize that for the magnetically insensitive CO lines, this disk continuum is the only fitted quantity that has any effect on the IR line profiles – all other key parameters come from the optical fits or literature data. An example fit is shown for the CTTS TW Hya in Figure 1. Note the obvious broadening of the 4 Ti I lines in the upper two panels of the figure and the lack of broadening seen in the CO lines of the lower panel. In Table 1 below we list the total magnetic flux, ΣBf (equal to the mean magnetic field), for each star.

3.2. Optical Spectropolarimetry

As discussed by Johns-Krull et al. (1999a), the He I 5876 Å emission line which forms in the accretion shock on the stellar surface is strongly circularly

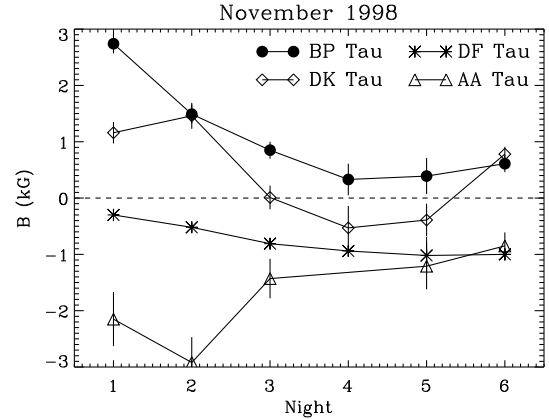


Fig. 3. Magnetic field measurements based on circular polarization detected in the He I emission line of 4 CTTS.

polarized in the CTTS BP Tau, while the photospheric absorption lines are not (Figure 2). In order to study the geometry of the magnetic field controlling the accretion, we observed the He I polarization in 4 CTTS (AA Tau, BP Tau, DF Tau, & DK Tau) over nearly an entire rotation cycle. The nightly He I polarization translated into a mean line of sight magnetic field is shown for each star in Figure 3. All 4 stars show significant, time variable circular polarization in their He I emission lines. In the stars with the best signal to noise (DF Tau – $P_{\text{rot}} = 8.5\text{d}$; DK Tau – $P_{\text{rot}} = 8.4\text{d}$; BP Tau – $P_{\text{rot}} = 7.6\text{d}$), the variations are smooth and nearly sinusoidal. This type of variation is similar to that caused by dipole magnetic fields in magnetic Ap stars (Wade et al. 1997). In contrast to the He I emission line, no significant polarization is detected in the photospheric absorption lines of the 4 CTTS.

4. DISCUSSION

The new IR data shows that for each TTS observed, the Ti I lines show excess broadening which can be well fit with a distribution of magnetic field strengths on the stellar surface. The magnetically insensitive CO lines show no excess broadening relative to that expected from a normal stellar photosphere, reinforcing the conclusion that the Ti I lines are tracing magnetic fields and not some other broadening mechanism such as Doppler broadening in a circumstellar disk.

The spectropolarimetry data show what appears to be rotational modulation of the magnetic field in the accretion shock (traced by He I) on 4 CTTS. This strongly suggests that accretion onto CTTS is indeed controlled by the stellar magnetic field as stated in magnetospheric accretion theory. The simple tem-

TABLE 1

TTS MAGNETIC FIELD MEASUREMENTS

Star	Type	B (kG) ^a	Data Type
BP Tau	K7 CTTS	2.1	IRB
DF Tau	M2 CTTS	2.3	IRB
DK Tau	M0 CTTS	2.7	IRB
Hubble 4	K7 NTTS	2.4	IRB
LkCa 15	K5 CTTS	1.1	EW
Tap 35	K1 NTTS	1.0	EW
T Tau	K0 CTTS	2.5,2.4	IRB,EW
TW Hya	K7 CTTS	2.6	IRB
BP Tau	K7 CTTS	2.8	Pol
DK Tau	M0 CTTS	1.5	Pol
AA Tau	M0 CTTS	2.9	Pol
DF Tau	M2 CTTS	1.0	Pol
TW Hya	K7 CTTS	2.1	Pol

^aFor polarimetry data types, the value represents the peak absolute field observed in the He I emission line. For all other types, the field is the average field in the photosphere.

poral behavior also suggests that the field component controlling the accretion has a relatively simple geometry, perhaps dipolar in nature. However, the lack of polarization observed in photospheric absorption lines shows that the field at the stellar surface is not dipolar. These are not necessarily contradictory statements. The dipole component of the magnetic field falls off the slowest with distance from the star. If the disk is truncated at several stellar radii, the dipole component of the field will likely dominate at this distance. This may force the accretion to proceed along dipole-like magnetic field lines, despite a confusing magnetic geometry present at the stellar surface.

Table 1 summarizes the current and historical results for magnetic field measurements on TTS. The *Data Type* column refers to the type of analysis done: IRB for detection of Zeeman broadening in high resolution IR spectra; EW for the detection of equivalent width enhancements in magnetically sensitive lines in the optical; Pol for the detection of circular polarization in the He I emission line.

Johns–Krull et al. (1999b) give field strength predictions from theory for 16 CTTS. At this time only 4 stars can be used for the comparison between theoretical and observed values. While the observed field strengths are generally of the right magnitude, there does not appear to be any correlation between the

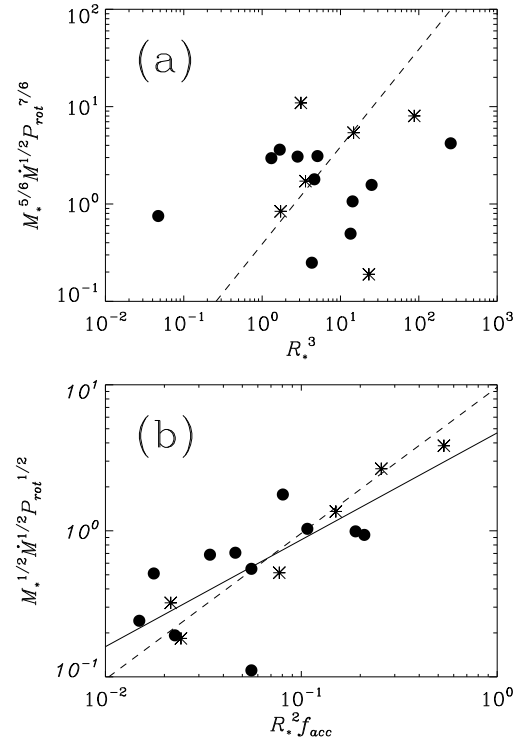


Fig. 4. (a) The top panel shows the quantity $(M_*/M_\odot)^{5/6}(\dot{M}/1 \times 10^{-7} M_\odot \text{yr}^{-1})^{1/2} P_{rot}^{7/6}$ versus $(R_*/R_\odot)^3$ for the sample of stars from VBJ. Single CTTSs are shown in solid circles while CTTSs in binary systems are shown in asterisks. The dashed line shows the best fit line whose slope (1.0) is predicted simple dipole theory. (b) The bottom panel shows the quantity $(M_*/M_\odot)^{1/2}(\dot{M}/1 \times 10^{-7} M_\odot \text{yr}^{-1})^{1/2} P_{rot}^{1/2}$ versus $(R_*/R_\odot)^2 f_{acc}$ for the sample of stars from VBJ. Plot symbols are the same as in panel (a). Shown in the solid line is the best fit line to the data, and shown in the dashed line is best fit line whose slope (1.0) is predicted by the trapped flux model.

observed and predicted magnetic field values. This may mean that our understanding of magnetospheric accretion is far from complete. On the other hand, the polarization measurements described above show that the mean photospheric fields on CTTS are not dipolar as assumed in the simple theories. These considerations led Johns–Krull and Gafford (2002) to re-examine the predictions of magnetospheric accretion theory. Looking at the mean photospheric field strengths given in Table 1, there is not much variation from star to star, with most values at ~ 2.5 kG. While the sample is small, this led Johns–Krull and Gafford (2002) to assume that the field strength is

essentially constant from one CTTS to the next, perhaps due to a dynamo limit operating in these fully convective stars. Then, for simple dipolar accretion theories, one would expect $R_*^3 \propto M_*^{5/6} \dot{M}^{1/2} P_{rot}^{7/6}$.

In their detailed study of magnetospheric accretion onto CTTS, Ostriker and Shu (1995) identified the trapped flux in the region of the disk truncation radius as the key quantity: independent of the magnetic field geometry on the stellar surface, a certain amount of magnetic flux near the inner edge of the disk is required to maintain equilibrium. Johns–Krull and Gafford (2002) used this notion to abandon the dipole field assumption, and showed that under any geometry, this trapped flux idea predicts that $R_*^2 f_{acc} \propto M_*^{1/2} \dot{M}^{1/2} P_{rot}^{1/2}$ where f_{acc} is the filling factor of accretion zones on the stellar surface. The observational study of Valenti, Basri, & Johns (1993 - VBJ) estimates all the parameters need to test these two relationships, which is shown in Figure 4. This figure clearly shows that the trapped flux idea of Ostriker and Shu (1995) can be combined with non-dipole field geometries to accurately predict the relationship between stellar mass, radius, rotation, and mass accretion in CTTS systems; whereas the simple dipolar assumption fails to make predictions supported by the data.

We wish to acknowledge generous support from the NASA Origins Program through grant NAG5-8098.

REFERENCES

- Basri, G., Marcy, G. W., & Valenti, J. A. 1992, *ApJ*, 390, 622
- Bertout, C. 1989, *ARAA*, 27, 351
- Bertout, C., Basri, G., & Bouvier, J. 1988, *ApJ*, 330, 350
- Borra, E. F., Edwards, G., & Mayor, M. 1984, *ApJ*, 284, 211
- Brown, D. N. & Landstreet, J. D. 1981, *ApJ*, 246, 899
- Camenzind, M. 1990, *Rev. Mod. Astron.*, 3, 234
- Cameron, A. C. & Campbell, C. G. 1993, *A&A*, 274, 309
- Donati, J.-F., Semel, M., Carter, B. D., Rees, D. E., & Cameron, A. C. 1997, *MNRAS*, 291, 658
- Ghosh, P. & Lamb, F. K. 1979, *ApJ*, 232, 259
- Greene, T. P., Tokunaga, A. T., Toomey, D. W., & Carr, J. C. 1993, *Proceedings SPIE*, 1946, 313
- Guenther, E. W., Lehmann, H., Emerson, J. P., & Staude, J. 1999, *A&A*, 341, 768
- Hauschildt, P. H., Allard, F., & Baron, E. 1999, *ApJ*, 512, 377
- Johns–Krull, C. M. & Gafford, A. D. 2002, *ApJ*, 573, 685
- Johns–Krull, C. M., Valenti, J. A., Hatzes, A. P., & Kanaan, A. 1999a, *ApJ*, 510, L41
- Johns–Krull, C. M., Valenti, J. A., & Koresko, C. 1999b, *ApJ*, 516, 900
- Koide, S., Shibata, K., & Kudoh, T. 1999, *ApJ*, 522, 727
- Königl, A. 1991, *ApJ*, 370, L39
- Ostriker, E. C. & Shu, F. H. 1995, *ApJ*, 447, 813
- Shu, F. H., Najita, J., Ostriker, E., Wilkin, F., Ruden, S., & Lizano, S. 1994, *ApJ*, 429, 781
- Tokunaga, A. T., Toomey, D. W., Carr, J. S., Hall, D. N. B., & Epps, H. W. 1990, *Proceedings SPIE*, 1235, 131
- Tull, R. G., MacQueen, P. J., Sneden, C., & Lambert, D. L. 1995, *PASP*, 107, 251
- Uchida, Y. & Shibata, K. 1984, *PASPJ*, 36, 105
- Valenti, J. A., Basri, G., & Johns, C. M. 1993, *AJ*, 106, 2024 (VBJ)
- Vogt, S. S. 1980, *ApJ*, 240, 567
- Vogt, S. S., Tull, R. G., & Kelton, P. W. 1980, *ApJ*, 236, 308
- Wade, G. A., Landstreet, J. D., Elkin, V. G., & Romanuk, I. I. 1997, *MNRAS*, 292, 748
- Wickramasinghe, D. T. & Ferrario, L. 2000, *New Astron. Rev.*, 44, 69